

Enumerative Methods in Quantum Electrodynamics

Ali Assem Mahmoud
 National Research Council of Canada, Digital Technologies
 Waterloo, ON, Canada.
ali.mahmoud@uwaterloo.ca

ABSTRACT. We show that observables in QED-type theories can be realized in terms of a combinatorial structure called chord diagrams. One advantage of this combinatorial representation is that it simplifies the study of the asymptotic behavior of corresponding Green functions. Particularly, using the new representation, there is no need to use the standard approach of singularity analysis. This relation also reveals the unexplained correlation between the number of Feynman diagrams in Yukawa theory and the diagrams in quenched QED.

1. Introduction and Setup

In perturbation theory, it is essential to study the behaviour of Green functions at large orders. This however usually depends on the problem of approximating the number of diagrams contributing to the perturbative terms, and, in that regards, it is shown in [7] that it suffices to consider the problem as a zero-dimensional field theory. In this paper we will establish a strong relation between 1PI Feynman diagrams in certain QED-type theories and a combinatorial structure called *chord diagrams*. Chord diagrams offer more simplicity when studying the respective generating functions at large orders. Moreover, the way these Feynman diagrams are mapped into chord diagrams is cryptic, which should probably mean that there is still more to highlight in this direction. This also gives rise to the question of why these graph-theoretic matchings are sufficient to represent the theory. The method used here is generic and can be applied to other QFT theories with a cubic-type vertex. We will regularly appeal to theorems about factorially divergent power series (see [1] or Appendix A in [10]). First we briefly set-up the context in perturbation theory. In most parts we follow the notation in [2] as we will need to compare some of the results eventually.

1.1. Zero-Dimensional Scalar Theories with Interaction. We are particularly considering quenched QED and Yukawa theory. These are examples of theories with interaction, where the partition function takes the form

$$Z(\hbar, j) := \int_{\mathbb{R}} \frac{1}{\sqrt{2\pi\hbar}} e^{\frac{1}{\hbar} \left(-\frac{x^2}{2} + V(x) + xj \right)} dx,$$

where an additional term is added to the potential, namely xj , with j called the *source*.

The generated Feynman diagrams are labeled, and hence in order to restrict ourselves to connected diagrams we have to take the logarithm of the partition function, commonly known as the *free energy*:

$$W(\hbar, j) := \hbar \log Z(\hbar, j),$$

which generates all connected diagrams.

As customary in QFT, to move to the *quantum effective action* G , which generates 1PI diagrams, one takes the Legendre transform of W :

$$(1.1) \quad G(\hbar, \varphi_c) := W - j\varphi_c,$$

where $\varphi_c := \partial_j W$. The coefficients $[\varphi_c^n]G$ are called the (*proper*) *Green functions* of the theory. Recall that from a graph-theoretic point of view, being *1PI* (1-particle irreducible) is another way of saying 2-connected. Thus, combinatorially, the Legendre transform, as in [9], is seen to be the transportation from connected diagrams to 2-connected or *1PI* diagrams. In that sense, the order of the derivative $\partial_{\varphi_c}^n G|_{\varphi_c=0} = [\varphi_c^n]G$ determines the number of external legs.

In the next part of the discussion, we shall need the following physical jargon and terminology:

- (1) The Green function $[\varphi_c^1]G = \partial_{\varphi_c} G|_{\varphi_c=0}$ generates all *1PI* diagrams with exactly one external leg, which are called the *tadpoles* of the theory (Figure 1).

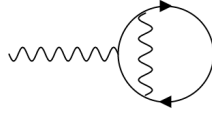


FIGURE 1. A tadpole diagram in QED

- (2) The Green function $[\varphi_c^2]G = \partial_{\varphi_c}^2 G|_{\varphi_c=0}$ generates all *1PI* diagrams with two external legs. Such a diagram is called a *1PI propagator* (can replace an edge in the theory; Figure 2).

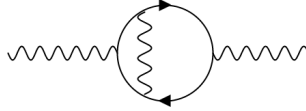


FIGURE 2. A propagator diagram

- (3) For $n > 2$, $\partial_{\varphi_c}^n G|_{\varphi_c=0} = [\varphi_c^n]G$ is called the *n-point function*.

In quenched QED, some of the quantities that we are going to compare their expansions with the generating series of 2-connected chord diagrams are the *renormalized* Green functions with respect to a chosen *residue*. We will not however digress into the Hopf-algebraic treatment of renormalization here. For more about this topic the reader can consult [11, 10], or the original paper by D. Kreimer and A. Connes [5].

2. *k*-Connected Chord Diagrams

DEFINITION 2.1 (Chord diagrams). A *chord diagram* on n chords (i.e. of size n) is geometrically perceived as a circle with $2n$ nodes that are matched into disjoint pairs, with each pair corresponding to a *chord*.

DEFINITION 2.2 (Rooted chord diagrams). A *rooted chord diagram* is a chord diagram with a selected node. The selected node is called the *root vertex*, and the chord with the root vertex is called the *root chord*. In other words, a rooted chord diagram of size n is a matching of the set $\{1, \dots, 2n\}$. For an algebraic definition, this is the same as a fixed-point free involution in S_{2n} . Then the generating series for rooted chord diagrams is

$$(2.1) \quad D(x) := \sum_{n=0}^{\infty} (2n-1)!! x^n$$

All chord diagrams considered here are going to be rooted and so, when we say a chord diagram we tacitly mean a rooted one.

Now, a rooted chord diagram can be represented in a linear order, by numbering the nodes in counterclockwise order, starting from the root which receives the label ‘1’. A chord in the diagram may be referred to as $c = \{a < b\}$, where a and b are the nodes in the linear order.

DEFINITION 2.3 (Intervals). In the linear form of a rooted chord diagram, an *interval* is the space to the right of one of the nodes in the linear representation. Thus, a rooted diagram on n chords has $2n$ intervals.

For example, this includes the space to the right of the last node (in linear order).

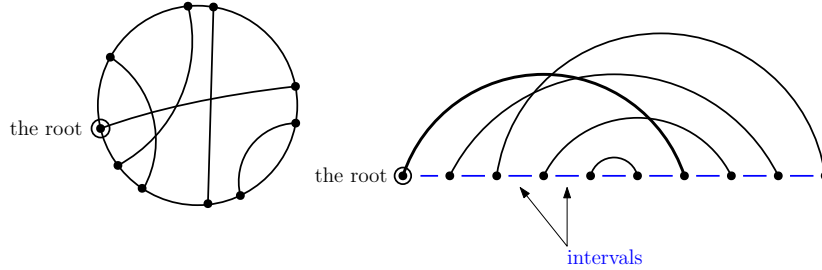


FIGURE 3. A rooted chord diagram and its linear representation

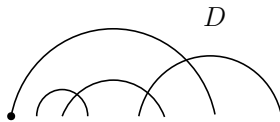
As may be expected by now, the crossings in a chord diagram encode much of the structure and so we ought to give proper notation for them. Namely, in the linear order, two chords $c_1 = \{v_1 < v_2\}$ and $c_2 = \{w_1 < w_2\}$ are said to *cross* if $v_1 < w_1 < v_2 < w_2$ or $w_1 < v_1 < w_2 < v_2$. Tracing all the crossings in the diagram leads to the following definition:

DEFINITION 2.4 (The Intersection Graph). Given a (rooted) chord diagram D on n chords, consider the following graph \mathcal{G}_D : the chords of the diagram will serve as vertices for the new graph, and there is an edge between the two vertices $c_1 = \{v_1 < v_2\}$ and $c_2 = \{w_1 < w_2\}$ if $v_1 < w_1 < v_2 < w_2$ or $w_1 < v_1 < w_2 < v_2$, i.e. if the chords *cross* each other. The graph so constructed is called the *intersection graph* of the given chord diagram.

REMARK 2.1. A labelling for the intersection graph can be obtained as follows: give the label 1 to the root chord; order the components obtained if the root is removed according to the order of the first vertex of each of them in the linear representation, say the components are C_1, \dots, C_n ; and then recursively label each of the components. It is easily verified that a rooted chord diagram can be uniquely recovered from its labelled intersection graph.

DEFINITION 2.5 (Connected Chord Diagrams). A (rooted) chord diagram is said to be *connected* if its intersection graph is connected (in the graph-theoretic sense). A *connected component* of a diagram is a subset of chords which itself forms a connected chord diagram. The term *root component* will refer to the connected component containing the root chord.

EXAMPLE 2.1. The diagram D below is a connected chord diagram in linear representation, where the root node is drawn in black.



The generating function for connected chord diagrams (in the number of chords) is denoted by $C(x)$. Thus $C(x) = \sum_{n=0} C_n x^n$, where C_n is the number of connected chord diagrams on n chords. The first terms of $C(x)$ are found to be

$$C(x) = x + x^2 + 4x^3 + 27x^4 + 248x^5 + \dots ;$$

the reader may refer to OEIS sequence [A000699](#) for more coefficients. The next lemma lists some classic decompositions for chord diagrams (see [8] for example).

LEMMA 2.1 ([8, 10]). *If $D(x), C(x)$ are the generating series for chord diagrams and connected chord diagrams respectively, then*

- (i) $D(x) = 1 + C(xD(x)^2)$,
- (ii) $D(x) = 1 + xD(x) + 2x^2D'(x)$, and
- (iii) $2xC(x)C'(x) = C(x)(1 + C(x)) - x$.

The main object we use throughout is chord diagrams with certain degrees (strengths) of connectivity.

DEFINITION 2.6 (*k*-Connected Chord Diagrams). A chord diagram on n chords is said to be *k*-connected if there is no set S of consecutive endpoints, with $|S| < 2n - k$, S is paired with less than k endpoints not in S (here we assume the endpoints are consecutive in the sense of the linear representation). In other words, the diagram requires the deletion of at least k chords to become disconnected. A *k*-connected diagram which is not $k + 1$ -connected will be said to have *connectivity k*.

The following relation between connected and 2-connected chord diagrams was established by the author in [10].

PROPOSITION 2.2 ([10]). *The following functional relation between connected and 2-connected diagrams holds:*

$$(2.2) \quad C = \frac{C^2}{x} - C_{\geq 2} \left(\frac{C^2}{x} \right).$$

The following corollary is about the asymptotic behaviour of $C_{\geq 2}(x)$. See [1] or Appendix A in [10] for more on factorially divergent power series and the terminology.

COROLLARY 2.3 ([10]). $C_{\geq 2}(x) \in \mathbb{R}[[x]]_{\frac{1}{2}}^2$ and $\left(\mathcal{A}_{\frac{1}{2}}^2 C_{\geq 2} \right)(x) = \frac{1}{\sqrt{2\pi}} \cdot \frac{x^2}{C_{\geq 2} S} \cdot e^{\frac{-1}{2x}[(S+x)^2-1]}$,

where $S(x) = \frac{1}{\left(1 - \frac{C_{\geq 2}(x)}{x}\right)}$ is the generating series for sequences of 2-connected chord diagrams counted by one less chord. Consequently, one computes that

$$(2.3) \quad (C_{\geq 2})_n = e^{-2}(2n-1)!! \left(1 - \frac{6}{2n-1} - \frac{4}{(2n-3)(2n-1)} - \frac{218}{3} \frac{1}{(2n-5)(2n-3)(2n-1)} - \frac{890}{(2n-7)(2n-5)(2n-3)(2n-1)} - \frac{196838}{15} \frac{1}{(2n-9)\cdots(2n-1)} - \cdots \right).$$

3. QED Theories, Quenched QED, and Yukawa Theory

The two theories that we consider here are quenched QED and Yukawa theory, which are examples of QED-type theories. In these theories we have two particles, namely, fermion and boson (wiggly and dashed edges) particles, and we have only three-valent vertices of the type fermion-fermion-boson. We will compute the asymptotics of $z_{\phi_c|\psi_c|^2}(\hbar_{\text{ren}})$ in quenched QED, as well as the asymptotics of the green functions $\partial_{\phi_c}^i (\partial_{\psi_c} \partial_{\bar{\psi}_c})^j G^{\text{Yuk}} \Big|_{\phi_c=\psi_c=0}$. The approach is completely combinatorial and depends on establishing bijections between the diagrams in the combinatorial interpretation of the considered series and different classes of chord diagrams. Unlike the approach applied in [2], we do not need to refer to singularity analysis nor the representation of $\mathcal{S}(x)$ by affine hyperelliptic curves.

3.1. The Partition Function. The partition function takes the form

$$(3.1) \quad Z(\hbar, j, \eta) = \int_{\mathbb{R}} \frac{1}{\sqrt{2\pi\hbar}} e^{\frac{1}{\hbar} \left(-\frac{x^2}{2} + jx + \frac{|\eta|^2}{1-x} + \hbar \log \frac{1}{1-x} \right)} dx.$$

We are not going to discuss the physical reasoning behind the above expression, the reader may refer to QFT books or surveys for more details, e.g. see [3]. We only hint that, combinatorially, $\hbar \log \frac{1}{1-x}$

generates fermion loops, while $\frac{|\eta|^2}{1-x}$ generates a fermion propagator. The special examples of Yukawa theory and quenched QED will be as follows:

- (1) Quenched QED is an approximation of QED where fermion loops are not present. So that the term $\hbar \log \frac{1}{1-x}$ does not appear in the partition function. Thus, the partition function for quenched QED is given by

$$Z^{QQED}(\hbar, j, \eta) = \int_{\mathbb{R}} \frac{1}{\sqrt{2\pi\hbar}} e^{\frac{1}{\hbar} \left(-\frac{x^2}{2} + jx + \frac{|\eta|^2}{1-x} \right)} dx.$$

- (2) For zero-dimensional Yukawa theory the partition function is just the integral in equation (3.1). That is, the partition function for zero-dimensional Yukawa theory is given by

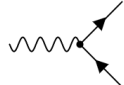
$$Z^{Yuk}(\hbar, j, \eta) = \int_{\mathbb{R}} \frac{1}{\sqrt{2\pi\hbar}} e^{\frac{1}{\hbar} \left(-\frac{x^2}{2} + jx + \frac{|\eta|^2}{1-x} + \hbar \log \frac{1}{1-x} \right)} dx.$$

In the next section we are going to display some of the literature on chord diagrams which will be essential for establishing the results.

4. Quenched QED

The case of quenched QED (QQED) was studied in [10], so we will only state the results here for the sake of completeness. We studied the counterterm $z_{\phi_c|\psi_c|^2}(\hbar_{ren})$ obtained in [2] (page 38). As mentioned earlier, QQED has a unique vertex type which is 3-valent. Hence, by [4], the series $z_{\phi_c|\psi_c|^2}(\hbar_{ren})$ enumerates the number of primitive quenched QED diagrams with vertex-type residue (see sequence A049464 of the OEIS for the first entries).

This is the same as counting the number of all diagrams γ with the following specifications:

- (1) two types of edges, fermion and boson (photon) edges, represented as \longrightarrow and $\sim\sim\sim$, respectively;
- (2) only three-valent vertices with the structure , with one fermion in, one fermion out, and one photon;
- (3) no fermion loops;
- (4) the residue $\text{res}(\gamma)$ is vertex-type; and
- (5) γ is 1PI primitive, in other words it is edge-connected and contains no subdivergences.

THEOREM 4.1 ([10]). *The generating series for the renormalization counterterms $z_{\phi_c|\psi_c|^2}(\hbar_{ren})$ and $z_{|\psi_c|^2}(\hbar_{ren})$ count 2-connected chord diagrams. More precisely,*

$$[\hbar_{ren}^{n-1}] z_{\phi_c|\psi_c|^2}(\hbar_{ren}) = [\hbar_{ren}^n] z_{|\psi_c|^2}(\hbar_{ren}) = [x^n] C_{\geq 2}(x).$$

This says that we can fathom the asymptotic behaviour of these counterterms by our knowledge of 2-connected chord diagrams, represented by Corollary 2.3. This gives

$$(4.1) \quad \begin{aligned} & [\hbar_{ren}^{n-1}] z_{\phi_c|\psi_c|^2}(\hbar_{ren}) = [\hbar_{ren}^n] z_{|\psi_c|^2}(\hbar_{ren}) = [x^n] C_{\geq 2}(x) = \\ & = e^{-2} (2n-1)!! \left(1 - \frac{6}{2n-1} - \frac{4}{(2n-3)(2n-1)} - \frac{218}{3} \frac{1}{(2n-5)(2n-3)(2n-1)} - \right. \\ & \left. - \frac{890}{(2n-7)(2n-5)(2n-3)(2n-1)} - \frac{196838}{15} \frac{1}{(2n-9)\cdots(2n-1)} - \cdots \right), \end{aligned}$$

which matches with the calculation through singularity analysis made in [2].

5. Yukawa Theory

In this section we will establish the connection between interacting Yukawa theory and chord diagrams. Unlike the case of quenched QED, the relation this time is well hidden. The problem was based on an observation, made by the author, upon seeing Table 18 (a) in [2] while working on the quenched QED case. For the sake of clarity, let us display Table 18 (a) of [2] (with an extra column added to emphasize the relation to chord diagrams):

		\hbar^0	\hbar^1	\hbar^2	\hbar^3	\hbar^4	\hbar^5	\hbar^6
1	$\partial_{\phi_c}^0 (\partial_{\psi_c} \partial_{\bar{\psi}_c})^0 G^{\text{Yuk}} \Big _{\phi_c=\psi_c=0}$	0	0	1/2	1	9/2	31	283
2	$\partial_{\phi_c}^1 (\partial_{\psi_c} \partial_{\bar{\psi}_c})^0 G^{\text{Yuk}} \Big _{\phi_c=\psi_c=0}$	0	1	1	4	27	248	2830
3	$\partial_{\phi_c}^2 (\partial_{\psi_c} \partial_{\bar{\psi}_c})^0 G^{\text{Yuk}} \Big _{\phi_c=\psi_c=0}$	-1	1	3	20	189	2232	31130
4	$\partial_{\phi_c}^0 (\partial_{\psi_c} \partial_{\bar{\psi}_c})^1 G^{\text{Yuk}} \Big _{\phi_c=\psi_c=0}$	-1	1	3	20	189	2232	31130
5	$\partial_{\phi_c}^1 (\partial_{\psi_c} \partial_{\bar{\psi}_c})^1 G^{\text{Yuk}} \Big _{\phi_c=\psi_c=0}$	1	1	9	100	1323	20088	342430

TABLE 1. The first coefficients of the proper Green functions $\partial_{\phi_c}^i (\partial_{\psi_c} \partial_{\bar{\psi}_c})^j G^{\text{Yuk}} \Big|_{\phi_c=\psi_c=0}$ of Yukawa theory such that $i + 2j \in \{0, 1, 2, 3\}$.

As we have mentioned in Section 3.1, Yukawa theory is different from quenched QED in that fermion loops are allowed in the diagrams. Thus, if \mathcal{U}_{ij} denotes the class of 1PI Feynman graphs counted by the Green function $\partial_{\phi_c}^i (\partial_{\psi_c} \partial_{\bar{\psi}_c})^j G^{\text{Yuk}} \Big|_{\phi_c=\psi_c=0}$, then, to our combinatorial concern, \mathcal{U}_{ij} consists of all graphs γ with the following specifications:

- (1) two types of edges (as before), fermion and boson (meson) edges, represented as \longrightarrow and ----- , respectively;
- (2) only three-valent vertices with the structure $\text{-----} \begin{array}{l} \nearrow \\ \searrow \end{array}$, with one fermion in, one fermion out, and one boson;
- (3) fermion loops are allowed;
- (4) the residue $\text{res}(\gamma)$ has i external boson legs, j external fermion-in legs, and j external fermion-out legs; and
- (5) γ is 1PI, i.e. it has no bridges (2-edge-connected). This is implied by the definition of proper Green functions.

Note that, unlike the quenched QED case, we are not restricting to primitive diagrams since we are not working with any expressions from renormalization in this part (yet).

LEMMA 5.1. *Let Γ be a Yukawa theory 1PI graph with $2j$ external fermion legs. Then*

$$(5.1) \quad |V(\Gamma)| = f + j,$$

where, as before, $|V(\Gamma)|$ is the number of vertices and f is the number of internal fermion edges.

PROOF. Consider the graph Γ' obtained from Γ by removing all boson edges and half edges. The resulting graph Γ' is generally a collection of fermion loops and fermion paths. The number of these paths should be j . Indeed, on one hand every such path will give two external fermion legs when the boson edges are present. To see this notice that, under the vertex condition, such paths can not end with a vertex: the boson edges can not then complete the degree of such a vertex. On the other hand, it is clear that the external fermion legs can only be at the ends of such paths.

As a consequence of the above argument, the number of vertices can be calculated as follows: every fermion loop has as many vertices as fermion edges. Whereas in every fermion path the number of vertices is more by one the number of internal fermion edges. This proves the lemma. \square

Next we investigate the combinatorial meaning of the Green functions in Table 1 and its relation to chord diagrams.

5.1. Yukawa Tadpole Graphs: $\partial_{\phi_c}^1 (\partial_{\psi_c} \partial_{\bar{\psi}_c})^0 G^{\text{Yuk}}(\hbar, \phi_c, \psi_c) \Big|_{\phi_c=\psi_c=0}$. By the definition mentioned earlier, $\partial_{\phi_c}^1 (\partial_{\psi_c} \partial_{\bar{\psi}_c})^0 G^{\text{Yuk}}(\hbar, \phi_c, \psi_c) \Big|_{\phi_c=\psi_c=0}$ is the generating series of Yukawa theory graphs with exactly one external leg, which is of boson type, graded by loop number. In other words,

$$[\hbar^n] \partial_{\phi_c}^1 (\partial_{\psi_c} \partial_{\bar{\psi}_c})^0 G^{\text{Yuk}} \Big|_{\phi_c=\psi_c=0}$$

is the number of *1PI* tadpole graphs with one boson leg and loop number n .

From Table 1, we can conjecture that $[\hbar^n] \partial_{\phi_c}^1 (\partial_{\psi_c} \partial_{\bar{\psi}_c})^0 G^{\text{Yuk}} \Big|_{\phi_c=\psi_c=0} = C_n$, the number of connected chord diagrams on n chords. Interestingly, unlike the quenched QED graphs, tadpoles do a great job hiding their chord diagrammatic structure. This however is to be unveiled Theorem 5.3 below. In Figure 6 below, we display the tadpoles counted in $[\hbar^4] \partial_{\phi_c}^1 (\partial_{\psi_c} \partial_{\bar{\psi}_c})^0 G^{\text{Yuk}} \Big|_{\phi_c=\psi_c=0}$, which, by our claim, should be 27 as C_4 .

REMARK 5.1. For the sake of simplicity of drawings, we will drop the direction of the fermion loops and assume it is always counter-clockwise. Besides, we will draw no more dashed boson lines, and shall instead use a light line for bosons and a heavier line for fermions. Note that the relative direction of loops matters in some cases and have to be compensated sometimes by a twist in the boson edges. For example, the following two tadpoles in Figure 4 are different, and shall be represented as in Figure 5:

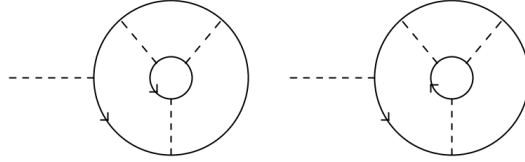


FIGURE 4. Two tadpoles may differ due to the relative orientation of fermion loops.

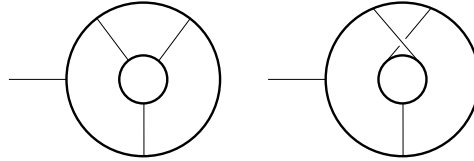


FIGURE 5. All loops are now assumed oriented counter-clockwise and the attached boson edges have to be twisted accordingly; Fermion edges are drawn thicker than boson edges.

The next lemma is a direct corollary to Lemma 5.1 for the case of tadpoles.

LEMMA 5.2. *For any Yukawa 1PI tadpole graph $\Gamma \in \mathcal{U}_{10}$ the following are true:*

- (1) *The number of vertices is equal to the number of fermion edges,*

$$|V(\Gamma)| = f.$$

- (2) *The number of all boson edges (including the external boson leg) is equal to the loop number of the graph. That is,*

$$p + 1 = \ell(\Gamma).$$

- (3) *Fermion loops partition the set of vertices;*

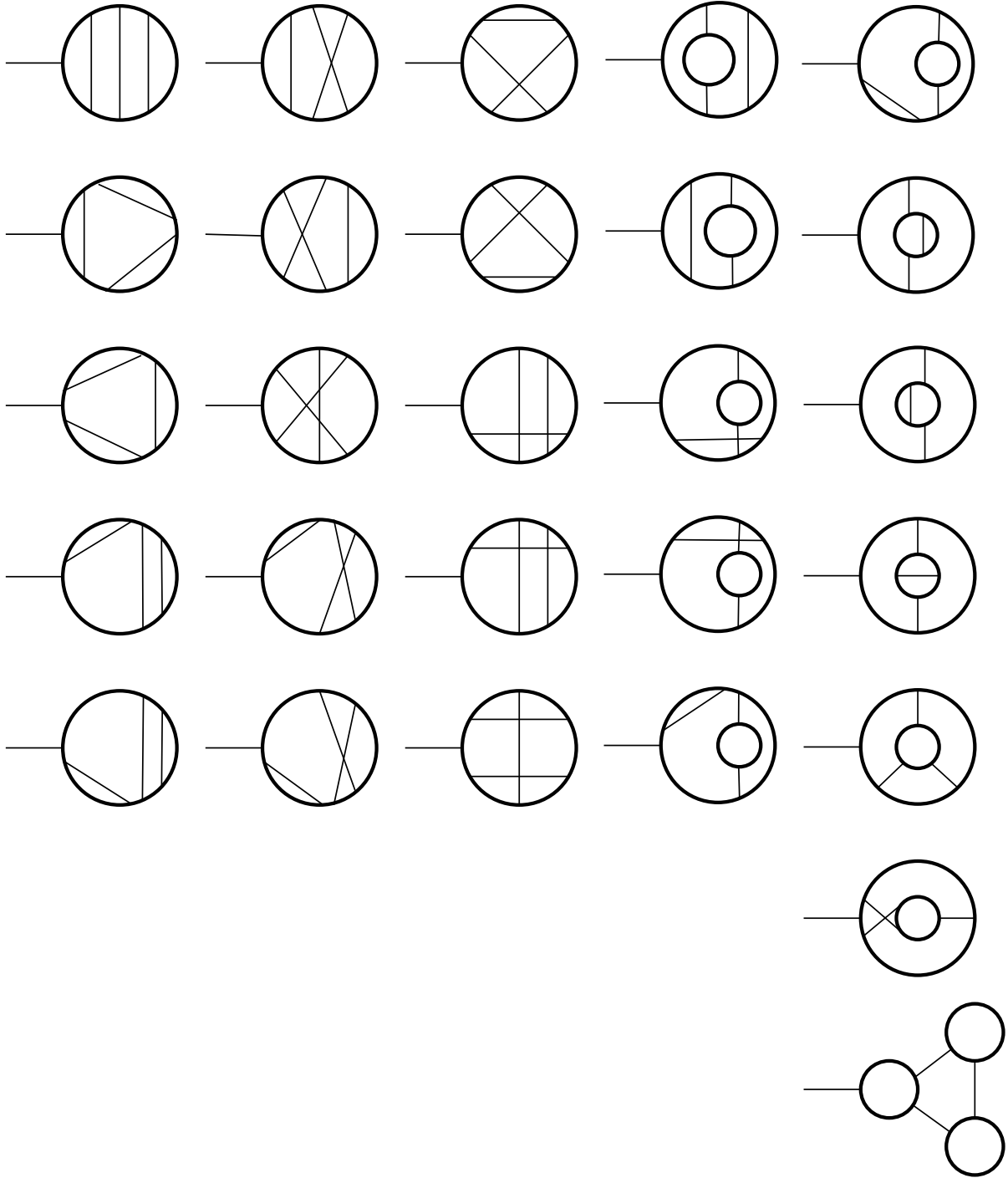


FIGURE 6. The 27 1PI tadpole graphs with loop number 4

where, as before, p is the number of internal boson edges (the p is suitable in this case too as it stands for a pion, pions are often the bosons in a Yukawa interaction), and f is the number of fermion edges (all fermion edges are internal in this case).

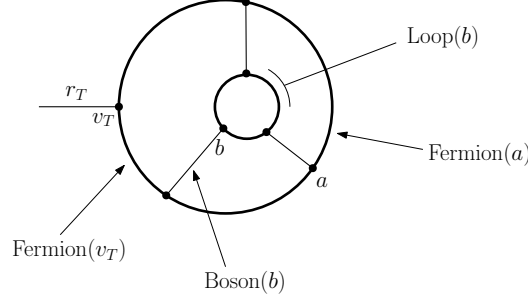
PROOF. By Lemma 5.1, we directly have $|V(\Gamma)| = f$. Euler's formula now implies

$$1 = |V(\Gamma)| - (p + f) + \ell(\Gamma) = f - (p + f) + \ell(\Gamma) = -p + \ell(\Gamma),$$

for any $\Gamma \in \mathcal{U}_{10}$. Finally, since there are no external fermion edges, every fermion edge must be on a fermion loop. Thus all vertices are on fermion loops, and by the condition on the vertices in the theory, no vertex can lie on more than one fermion loop. \square

Lemma 5.2 is useful in that we do not have to think about the loop number in proving the bijection to connected chord diagrams, and can instead focus on the more evident count of boson edges.

NOTATION 5.1. For a tadpole $T \in \mathcal{U}_{10}$, we will fix the notation that the external boson leg is denoted by r_T , and the vertex at the leg is denoted by v_T (this is consistent with the notation used in the previous section). For a vertex $a \in V(T)$ we let $\text{Loop}(a)$ denote the unique fermion loop containing a , and we let $\text{Fermion}(a)$ be the fermion edge coming out of a (i.e. the next on $\text{Loop}(a)$ counter-clockwise). $\text{Boson}(a)$ will denote the unique boson edge to which a is incident.



In the next proof we consider the free end of r to be a vertex of degree 1. Then the number of vertices is twice the number of boson edges.

THEOREM 5.3. *The number of Yukawa 1PI tadpole graphs with loop number n is equal to the number of connected chord diagrams on n chords. In other words,*

$$[\hbar^n] \partial_{\phi_c}^1 (\partial_{\psi_c} \partial_{\bar{\psi}_c})^0 G^{Yuk} |_{\phi_c = \psi_c = 0} = C_n.$$

PROOF. Let $T(x)$ be the generating series for tadpoles in \mathcal{U}_{10} , counted by the number of boson edges (including the external boson leg). We are taking advantage of Lemma 5.2 in order to use the number of bosons instead of the loop number. The theorem shall be proven through an algorithm that shows that $T(x)$ obeys the same recurrence as $C(x)$ (see Lemma 2.1), namely

$$2xT(x)T'(x) = T(x)^2 + T(x) - x.$$

First notice that the LHS stands for two tadpole diagrams, one of which has a distinguished end point of one of the boson edges (hence the 2 factor). For simplicity, we will treat the free end of an external boson leg as a vertex. Then let \mathcal{U}_{10}^\bullet be the class of tadpoles with a distinguished vertex. Also let $\mathcal{U}_{10} - \{\mathcal{X}\}$ be the class of tadpoles excluding \mathcal{X} , the tadpole with one vertex (\mathcal{X} has only the boson leg).

Let T_1, T_2 be tadpole graphs in \mathcal{U}_{10} , and assume that T_2 has a distinguished vertex d . By Notation 5.1, we let r_1 and r_2 be the boson legs of T_1 and T_2 , and we let v_1 and v_2 be the 3-valent vertices incident to r_1 and r_2 , respectively. Figure 7 illustrates the notation.

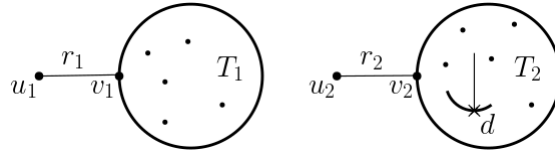


FIGURE 7. Notation for $(T_1, (T_2, d))$

Now we can describe the reversible algorithm as follows:

Algorithm Ψ : $(\mathcal{U}_{10} \times \mathcal{U}_{10}^\bullet) \longrightarrow (\mathcal{U}_{10} \times \mathcal{U}_{10}) \cup (\mathcal{U}_{10} - \{\mathcal{X}\})$

Input: $(T_1, (T_2, d)) \in (\mathcal{U}_{10} \times \mathcal{U}_{10}^\bullet)$, with notation as described above.

(a) If $d = u_2$ just **return** (T_1, T_2) .

(b) If $d \neq u_2$, do the following:

Move (counter-clockwise) along $\text{Loop}(v_1)$ in T_1 , determine $\text{Fermion}(v_1)$ and let w be the first vertex met on the loop. Note that w may be v_1 itself.

- (1) If $w = v_1$, i.e. T_1 contains no internal boson edges, **return** the tadpole T obtained as follows:
 - (i) Insert vertex v_1 together with the leg r_1 into $\text{Fermion}(d)$ in T_2 by making a subdivision of $\text{Fermion}(d)$.
 - (ii) Insert u_2 into the new $\text{Fermion}(v_1)$ on $\text{Loop}(d)$.
- (2) If $w \neq v_1$, **return** the tadpole T obtained as follows:
 - (i) Insert u_2 into $\text{Fermion}(v_1)$ in T_1 .
 - (ii) Detach w from $\text{Loop}(v_1)$ and insert it into $\text{Fermion}(d)$ in T_2 .

Figures 8 and 9 illustrate the two cases for (b).

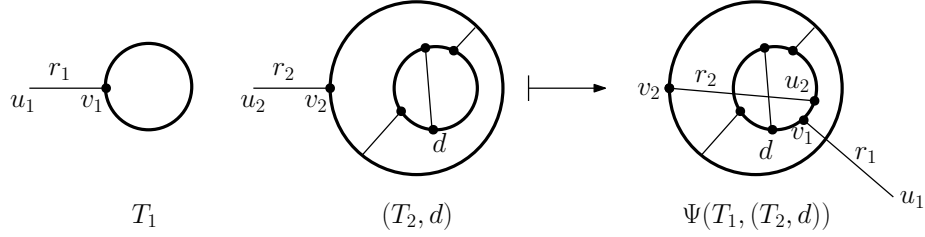


FIGURE 8. $\Psi(T_1, (T_2, d))$ when T_1 has exactly one vertex, the case $w = v_1$.

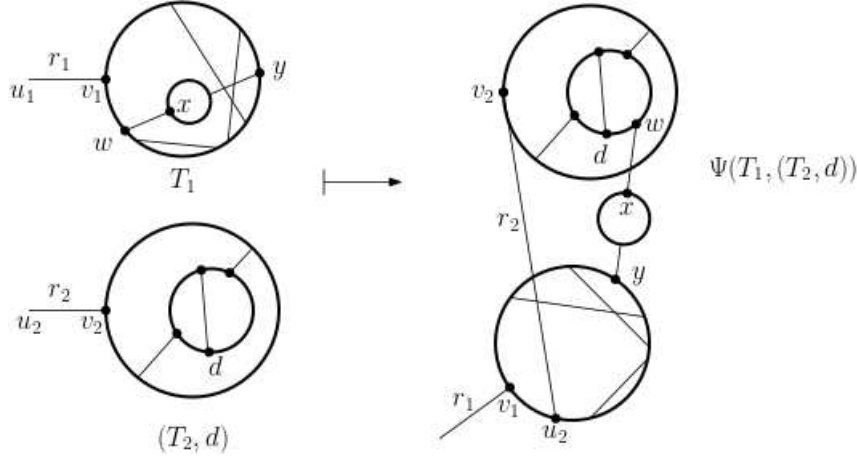


FIGURE 9. $\Psi(T_1, (T_2, d))$ for a general T_1 , the case $w \neq v_1$.

For the reverse process we can devise the following algorithm.

Algorithm Ψ^{-1} : $(\mathcal{U}_{10} \times \mathcal{U}_{10}) \cup (\mathcal{U}_{10} - \{\mathcal{X}\}) \longrightarrow (\mathcal{U}_{10} \times \mathcal{U}_{10}^\bullet)$

Input: $(T_1, T_2) \in (\mathcal{U}_{10} \times \mathcal{U}_{10})$, or $T \in \mathcal{U}_{10} - \{\mathcal{X}\}$

(a) If the input is a pair (T_1, T_2) then **return** $(T_1, (T_2, v_2))$.

- (b) If the input is a tadpole graph $T \in \mathcal{U}_{10} - \{\mathcal{X}\}$, do the following:
- (1) Move (counter-clockwise) along $\text{Loop}(v_T)$, determine the first vertex a met on the loop. Note that $a \neq v_T$ since we are excluding the tadpole with a single vertex.
 - (2) Determine the other end vertex of $\text{Boson}(a)$ and denote it by v_2 .
 - (3) Remove the vertex a from T and keep the resulting boson leg attached at v_2 . Let the resulting graph be denoted by Γ .
 - (4) Check whether Γ contains a bridge:
 - Case 1: If Γ is 2-edge-connected (i.e. contains no bridges) do
 - (1) Determine the first vertex on $\text{Loop}(v_T)$ before v_T , denote it by d .
 - (2) Remove v_T and its boson leg r_T . Denote the remaining tadpole by T_2 .
 - (3) **Return** $(\mathcal{X}, (T_2, d))$.
 - Case 2: If b_0 is a bridge (must be a boson edge) in Γ , undergo the following:
 - (1) Set $G = \Gamma$ and $b = b_0$.
 - (2) **{while** G has a bridge g **do**
 - (A) reset $b \leftarrow g$;
 - (B) determine the component γ that contains v_2 if b is removed;
 - (C) reset $G \leftarrow \gamma$.}
 - (3) Let w be the end vertex of b that lies in G . Notice that, after the while-loop, G contains no bridges.
 - (4) Determine the first vertex on $\text{Loop}(w)$ before w , denote it by d .
 - (5) Detach w from $\text{Loop}(d)$ in G and insert into $\text{Fermion}(v_T)$ (i.e. next to v_T on $\text{Loop}(v_T)$).
 - (6) Let $T_2 = G - w$ be the tadpole obtained from G after w is removed.
 - (7) Let T_1 be that tadpole obtained in $\Gamma - G$ after w is inserted on $\text{Loop}(v_T)$.
 - (8) **Return** $(T_1, (T_2, d))$.

Before discussing the algorithms, the reader may like to see Example 5.1 for applying Ψ^{-1} to $\Psi(T_1, (T_2, d))$ from Figure 9.

Now, for Algorithm Ψ , the two cases (a) and (b) are clearly distinguishable by the types of their outputs, so Let us focus on (b).

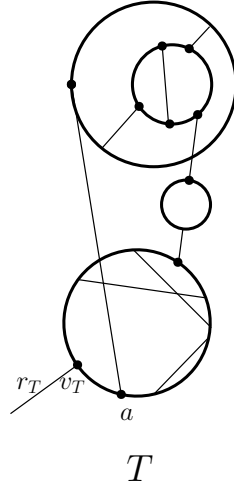
- (1) The special case in $(\Psi \text{ b:}(1))$ when $w = v_1$ returns a tadpole without bridges. Indeed, we only added an external leg r_1 at the position determined by d , and then we inserted the free end u_2 (the external leg of T_2). None of these steps changes the connectivity of T_2 , and the return value is indeed in $\mathcal{U}_{10} - \{\mathcal{X}\}$.
- (2) In $(\Psi \text{ b:}(2))$, when $w \neq v_1$, the result has no bridges, since what we do is roughly joining T_1 and T_2 by means of two boson edges in a certain way. Thus the result is indeed a tadpole in $\mathcal{U}_{10} - \{\mathcal{X}\}$. Notice that the first of these joints is attached next to the leg, and its removal leaves the graph with a bridge. This is of most importance in the reverse process.

Then, for Algorithm Ψ^{-1} , we have the following:

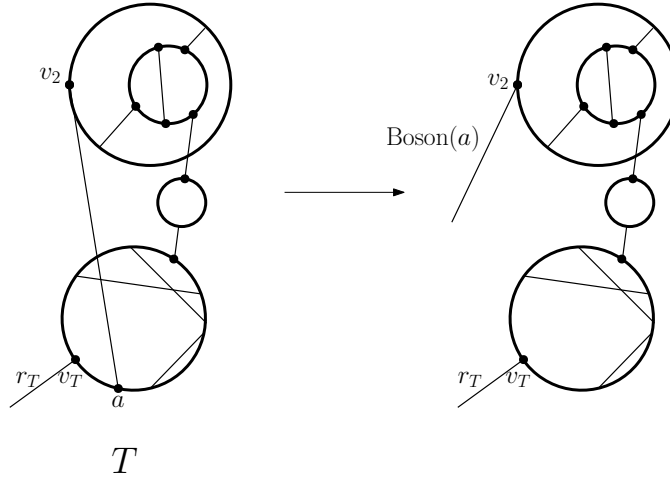
- (1) If the input is a pair, then this uniquely means that the distinguished vertex satisfies $d = u_2$.
- (2) If the input is a tadpole that stays bridgeless after the the vertex a next to v_T is removed then this uniquely means that $T_1 = \mathcal{X}$. Indeed, we have seen above that in all the other cases we get a bridge if the first boson edge after the external leg is removed.
- (3) If the input reveals a bridge b_0 when $\text{Boson}(a)$ is removed, then we learn that a and $\text{Boson}(a)$ formed the external leg of T_2 and we start disentangling T_2 from the graph. Roughly speaking, we need to determine d by using the fact that, in the absence of $\text{Boson}(a)$, $\text{Boson}(d)$ is a bridge coming from T_1 . The while loop in the algorithm works on finding the last such bridge.
- (4) By the engineering of the while-loop, the graph G obtained at the end of the loop has no more bridges, besides, it carries the traces of the last bridge b , which determines the distinguished vertex d .
- (5) After modifying G by removing w we get (T_2, d) , and simultaneously we get T_1 from the remaining graph by attaching w into $\text{Fermion}(v_T)$. By doing so, T_1 is also bridgeless.

This proves the theorem. □

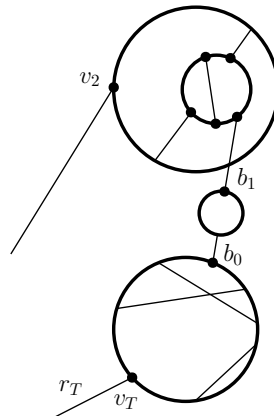
EXAMPLE 5.1. Let us apply Algorithm Ψ^{-1} to the tadpole T given in Figure 9 by



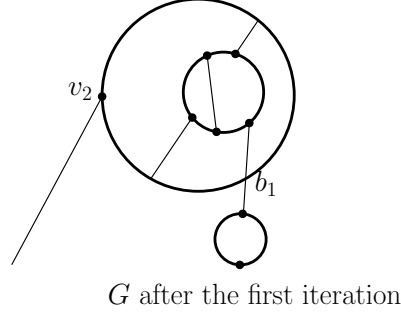
- (1) The input is a tadpole in $\mathcal{U}_{10} - \{\mathcal{X}\}$ and so we apply (b).
- (2) We determine a as the vertex next to v_T on $\text{Loop}(v_T)$, and with it we determine v_2 , the other end of $\text{Boson}(a)$.
- (3) We remove vertex a from T and keep $\text{Boson}(a)$ attached at v_2 as in the figure below.



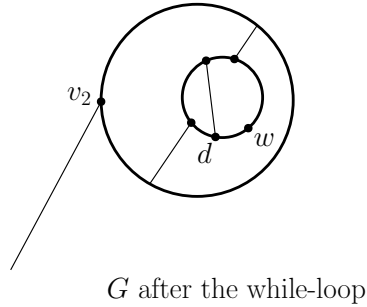
- (4) We check for bridges and we find one of them, we assume that our search provided the bridge b_0 .



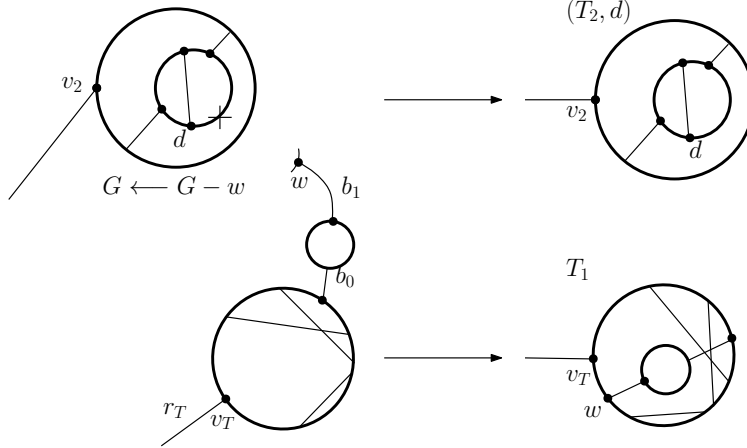
- (5) We enter the while loop with $G = \Gamma$ given above and $b = b_0$:
 (a) After the first iteration G is modified to be



- (b) Now G again has a bridge b , and, after the second iteration G has no more bridges. After the while-loop $b = b_1$ and G is given by



- (c) Finally, detach w from G , set $T_2 = G - w$, reset $G = G - w$, and insert w next to v_T in $\Gamma - G$ to get T_1 . The result is shown in the figure below.



Theorem 5.3 tells us that the two structures, Yukawa 1PI tadpoles and connected chord diagrams satisfy the same recurrence and hence there exists a bijection between the two classes obtained recursively. However, we still have to do one more bit of work to express this bijection. The bijection should respect the sizes, that is, a Yukawa 1PI tadpole with n boson edges (with n loops) should be mapped to a connected chord diagram on n chords.

Moreover, as we can see, the vertices of a tadpole should correspond to the vertices in a connected chord diagram, and the fermion edges should accordingly correspond to the intervals. It has not been made clear so far how we can order fermion edges in a way that resembles the natural linear order of the intervals in chord diagrams, an order that is compatible with the decomposition in Theorem 5.3. Definition 5.2 below addresses this issue. To see why the order should be defined this way, we have to

first recall the root share decomposition of connected chord diagrams. The root share decomposition has been used in the proof of Lemma 2.1, and now we need to define it properly:

DEFINITION 5.1 (Root Share Decomposition). The *root share decomposition* is the map $\nabla : \mathcal{C} \rightarrow \mathcal{C} \times (\mathcal{C}, \mathbb{N})$ defined by

$$\nabla C = (C_1, (C_2, k)),$$

where $1 \leq k \leq |C_2| - 1$, and C_1, C_2 are obtained as follows: Among the components produced by removing the root of C , C_2 is taken to be the first in intersection order with the root. k determines the interval in C_2 through which the root used to pass. C_1 is then obtained by removing the chords of C_2 from C .

If $(C_1, (C_2, k)) \in \mathcal{C} \times (\mathcal{C}, \mathbb{N})$ is a valid triplet then $\nabla^{-1}(C_1, (C_2, k))$ is the connected chord diagram obtained by placing C_1 in the k th interval of C_2 and pulling the root of C_1 out to become the root of the whole diagram (i.e. place it to the left of the root of C_2). See Figure 10.

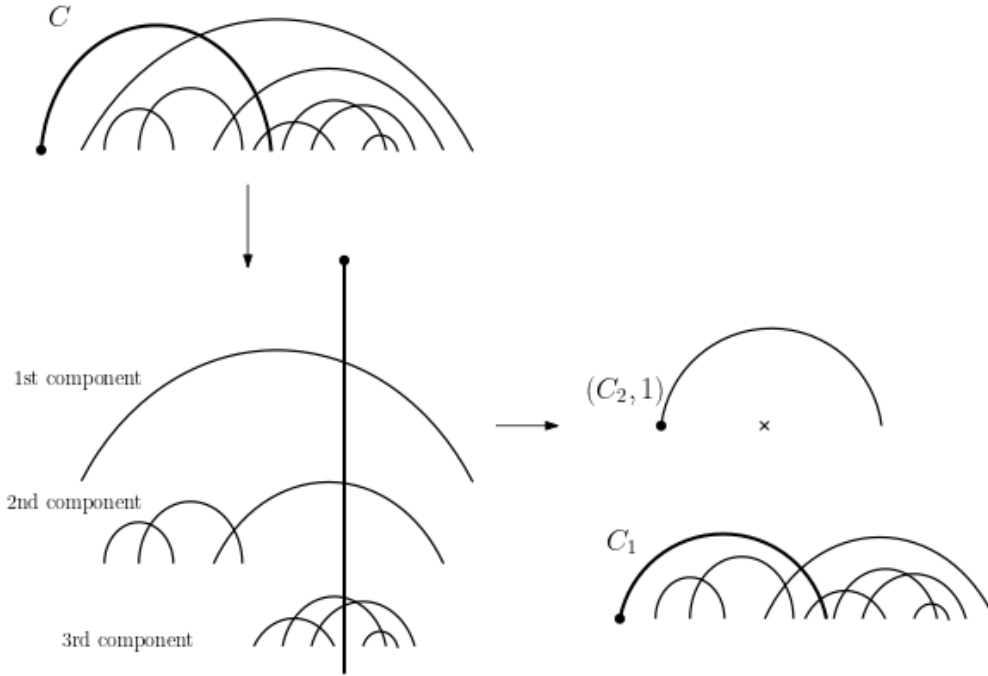


FIGURE 10. Root share decomposition of a connected chord diagram

The effect of the root share decomposition on the linear order of the intervals in C_1 and C_2 leads us to the following order on fermion edges in a Yukawa 1PI tadpole.

DEFINITION 5.2 (The Ψ -order). We define the Ψ -order on the fermion edges in a Yukawa 1PI tadpole inductively on the size n of the tadpoles as follows:

- * For a fermion edge e in a tadpole T , its Ψ -order takes values in \mathbb{N} and is to be denoted by $\psi_T(e)$.
 - For \mathcal{X} the unique fermion edge is ordered as 1.
 - Assume all tadpoles of size less than n are ordered and let T be a tadpole of size n . To order T do the following:
 - (1) Apply Ψ^{-1} to T to determine a triplet $(T_1, (T_2, d))$. As before, let v_T, v_1 and v_2 be the leg vertices in T, T_1 and T_2 respectively. Let w_1 be the vertex next to v_1 in T_1 . Also let w_T be the vertex in T next to v_T , and let w_d be the vertex in T next to the vertex d (i.e. these are the vertices of subdivisions created by Ψ). Note that $w_d = v_T$ if $T_1 = \mathcal{X}$.

(2) By the induction hypothesis it is assumed that we know the Ψ -ordering of T_1 and T_2 . Let

$$M = \max_{e \in T_1} \psi_{T_1}(e).$$

Case 1: $T_1 = \mathcal{X}$. Set $\psi_T(\text{Fermion}(v_T)) = 1$, and for any other fermion edge e in T define $\psi_T(e)$ such that

- (a) $\psi_T(e) = \psi_{T_2}(e) + 1$ if $e \in T_2$ and $\psi_{T_2}(e) < \psi_{T_2}(\text{Fermion}(d))$.
- (b) $\psi_T(\text{Fermion}(d)) = \psi_{T_2}(\text{Fermion}(d)) + 1$ (in T this is the dv_T edge).
- (c) $\psi_T(\text{Fermion}(w_T)) = \psi_{T_2}(\text{Fermion}(d)) + 2$.
- (d) $\psi_T(e) = \psi_{T_2}(e) + 2$ if $e \in T_2$.

Case 2: $T_1 \neq \mathcal{X}$. Set $\psi_T(\text{Fermion}(v_T)) = 1$, and for any other fermion edge e in T define $\psi_T(e)$ such that

- (a) $\psi_T(e) = \psi_{T_2}(e) + 1$ if $e \in T_2$ and $\psi_{T_2}(e) < \psi_{T_2}(\text{Fermion}(d))$.
- (b) $\psi_T(\text{Fermion}(d)) = \psi_{T_2}(\text{Fermion}(d)) + 1$ (in T this is the dw_2 edge).
- (c) $\psi_T(\text{Fermion}(w_T)) = \psi_{T_1}(\text{Fermion}(w_1)) + \psi_{T_2}(\text{Fermion}(d))$.
- (d) $\psi_T(e) = \psi_{T_1}(e) + \psi_{T_2}(\text{Fermion}(d))$ if $e \in T_1$.
- (e) $\psi_T(\text{Fermion}(w_d)) = M + \psi_{T_2}(\text{Fermion}(d)) + 1$.
- (f) $\psi_T(e) = \psi_{T_2}(e) + M + 1$ if $e \in T_2$.

EXAMPLE 5.2. Two examples of the Ψ -order are given in Figures 11 and 12. In Figure 13 we give the corresponding chord diagram for the tadpole in Figure 12. It is worth noticing how the two orders are constructed similarly.

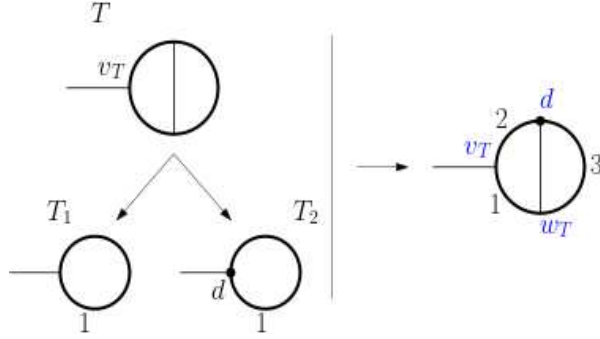


FIGURE 11. An example of the Ψ -order Case 1.

Now we can finally express the bijection between Yukawa 1PI tadpoles and connected chord diagrams.

If we use a vertex to indicate an interval in a chord diagram, then we mean, as usual, the interval to the right of the vertex in the linear representation. Analogously we use the fermion edge that comes next to a vertex in counter-clockwise direction. Also note that the interval in the root share decomposition can not be the rightmost interval of the diagram.

5.1.1. An Explicit Bijection.

COROLLARY 5.4. *Theorem 5.3 can be used to give an explicit bijection Λ between Yukawa theory 1PI tadpoles in (the class \mathcal{U}_{10}) and \mathcal{C} , the class of connected chord diagrams. Namely, $\Lambda : \mathcal{U}_{10} \rightarrow \mathcal{C}$ is defined recursively as follows:*

$$\Lambda(\mathcal{X}) = \text{---} \curvearrowright \text{---}; \quad \text{and}$$

$$\Lambda(T) = \nabla^{-1}(\Lambda(T_1), (\Lambda(T_2), \psi(d))),$$

where $\Psi^{-1}(T) = (T_1, (T_2, d))$, and, as defined earlier, $\mathcal{X} = \text{---} \bigcirc$.

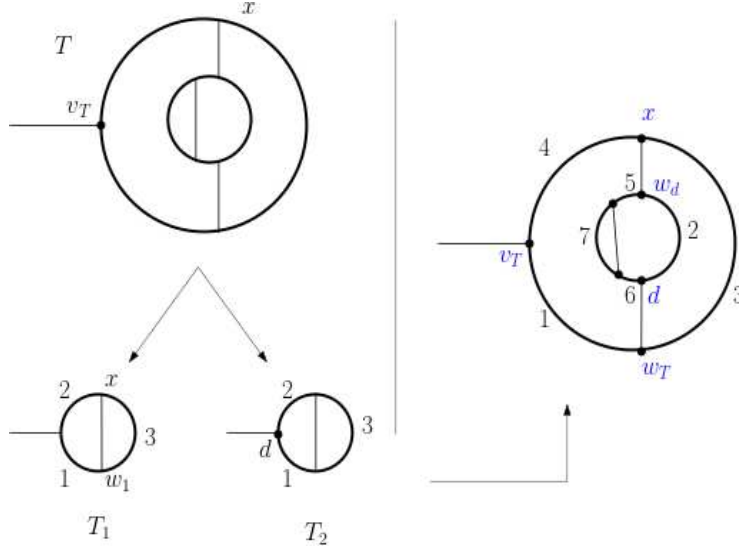


FIGURE 12. An example of the Ψ -order Case 2.

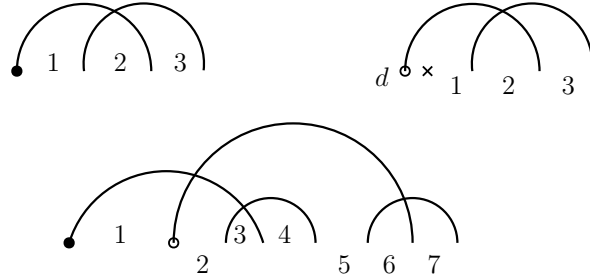


FIGURE 13. The corresponding chord diagrams for the graphs of Example 5.2, in Figure 12.

PROOF. The proof is straightforward from the definitions of the maps involved. The map is well defined by the uniqueness of the root share decomposition, and is a bijection since ψ , Ψ , and ∇ are bijections. \square

EXAMPLE 5.3. Figure 14 below illustrates all the steps from a tadpole T to its corresponding connected chord diagram. Namely, as the corollary states, given a Yukawa 1PI tadpole T , the process can be described as follows:

- (1) Use Ψ^{-1} to decompose T all the way down to copies of \mathcal{X} , with extra information about positions d_i at each step
- (2) Go up again step by step and use the recursive definition of ψ to order all the fermion edges in the graph.
- (3) Again start from the bottom to create the corresponding chord diagrams using ∇^{-1} and the values $\psi(d)$. The last insertion up gives $\Lambda(T)$.

REMARK 5.2. It is surprising that, in light of the result in [6], the bijection between Yukawa 1PI tadpoles and connected chord diagrams gives a bijection between Yukawa 1PI tadpoles and rooted bridgeless combinatorial maps. This will be investigated in future work.

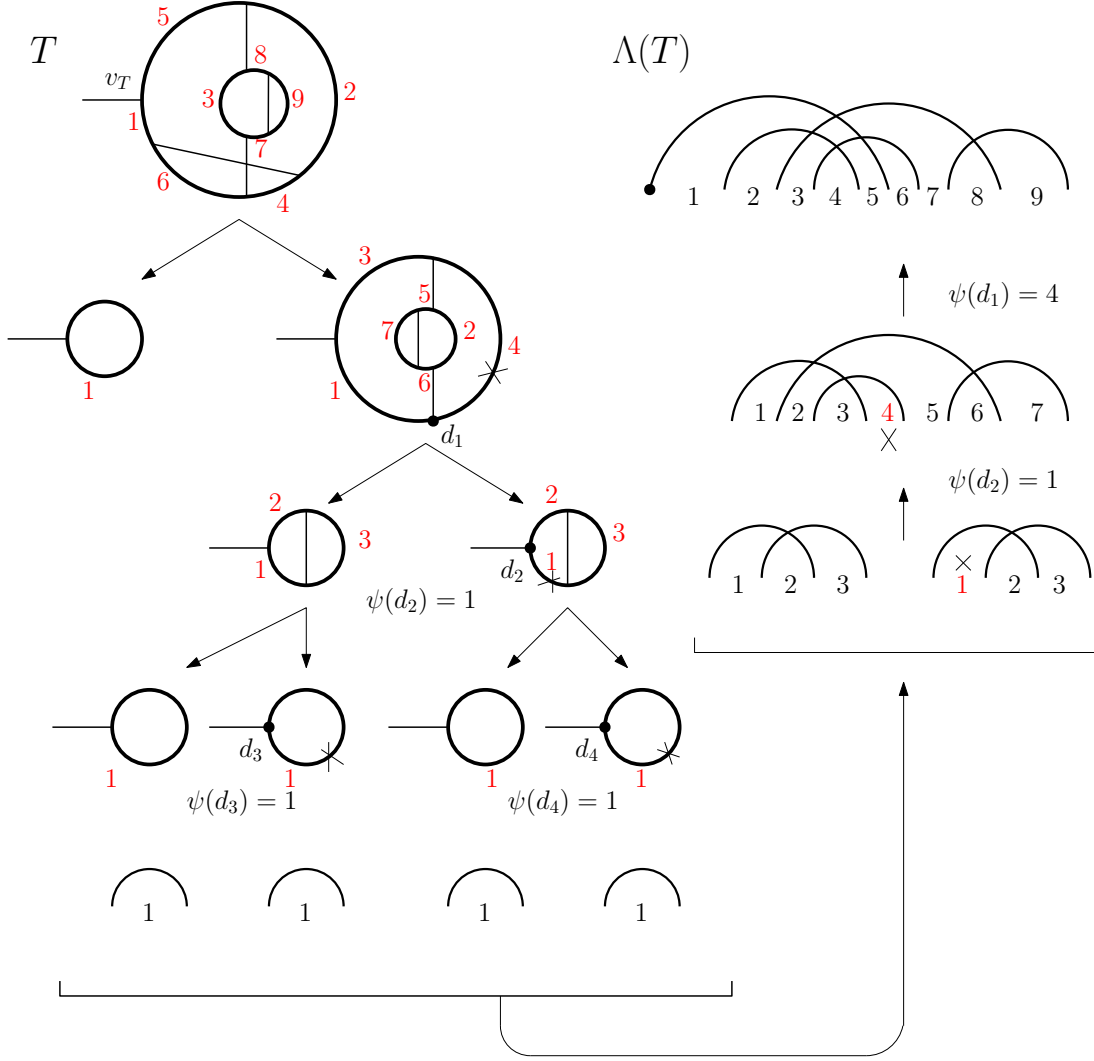


FIGURE 14. A complete example of the recursive calculation of Λ .

5.2. Yukawa Vacuum Graphs: $\partial_{\phi_c}^0 (\partial_{\psi_c} \partial_{\bar{\psi}_c})^0 G^{\text{Yuk}}(\hbar, \phi_c, \psi_c) \Big|_{\phi_c = \psi_c = 0}$. Here we interpret line 1 in Table 1. By definition, $\partial_{\phi_c}^0 (\partial_{\psi_c} \partial_{\bar{\psi}_c})^0 G^{\text{Yuk}}(\hbar, \phi_c, \psi_c) \Big|_{\phi_c = \psi_c = 0}$ generates all 1PI Yukawa graphs with no external legs. In physics jargon these are called vacuum graphs.

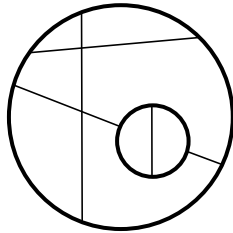


FIGURE 15. A 1PI vacuum graph in Yukawa theory.

By Lemma 5.1 we know that for a vacuum graph Γ we will still have $|V(\Gamma)| = f$, the number of internal fermion edges. Consequently, we also still get $p = \ell(\Gamma) - 1$ and $|V(\Gamma)| = 2p$ (Euler's formula

for the first), where p is the number of internal boson edges. Let $V(x)$ be the generating series of 1PI Yukawa vacuum graphs counted by the number of boson edges.

Before giving the chord-diagrammatic interpretation notice that in Table 1 we have

$$[\hbar^0] \partial_{\phi_c}^0 (\partial_{\psi_c} \partial_{\bar{\psi}_c})^0 G^{\text{Yuk}}(\hbar, \phi_c, \psi_c) \Big|_{\phi_c=\psi_c=0} = [\hbar^1] \partial_{\phi_c}^0 (\partial_{\psi_c} \partial_{\bar{\psi}_c})^0 G^{\text{Yuk}}(\hbar, \phi_c, \psi_c) \Big|_{\phi_c=\psi_c=0} = 0,$$

since we do not consider the empty graph or the plain loop to be 1PI graphs. The following proposition proves this conjecture and is a consequence of Theorem 5.3.

PROPOSITION 5.5. *Let $V(x)$ be the generating series of 1PI Yukawa vacuum graphs counted by the number of boson edges. Then*

$$V(x) = \frac{C(x)^2}{2x},$$

which implies that

$$[\hbar^{n+1}] \partial_{\phi_c}^0 (\partial_{\psi_c} \partial_{\bar{\psi}_c})^0 G^{\text{Yuk}}(\hbar, \phi_c, \psi_c) \Big|_{\phi_c=\psi_c=0} = [x^n] \frac{C(x)^2}{2x}.$$

PROOF. Let \mathcal{U}_{00} be the class of Yukawa 1PI vacuum graphs. It is clear that $\mathcal{U}_{10} - \{\mathcal{X}\} = X * \mathcal{U}_{00}^\bullet$, where \mathcal{U}_{00}^\bullet is the class of vacuum graphs with a distinguished fermion edge (or equivalently, with a distinguished vertex), and X as usual is used for the single constituent whose generating function is x (in this case it refers to an external boson edge to be inserted). Also note that our vacuum graphs must have at least one boson edge (the plain fermion loop is not considered 1PI).

Since there are two vertices for each chosen boson edge, we have that the generating function for \mathcal{U}_{00}^\bullet is

$$2xV'(x).$$

Thus, by Theorem 5.3, we should have

$$C(x) - x = 2x^2V'(x).$$

Then, by Lemma 2.1 we know that $2xC(x)C'(x) = C^2 + C - x$, and we get

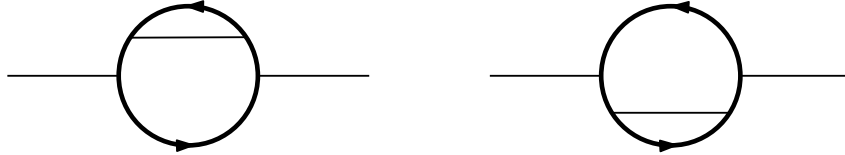
$$V'(x) = \frac{1}{2x^2}(C(x) - x) = \frac{1}{2x^2}(2xC(x)C'(x) - C(x)^2) = \frac{1}{2} \frac{(x(C(x)^2))' - C(x)^2}{x^2},$$

which can then be integrated to give the result. \square

5.3. Yukawa Graphs from $\partial_{\phi_c}^2 (\partial_{\psi_c} \partial_{\bar{\psi}_c})^0 G^{\text{Yuk}}(\hbar, \phi_c, \psi_c) \Big|_{\phi_c=\psi_c=0}$. The Yukawa 1PI graphs counted by loop number in line 3 of Table 1 are the graphs with exactly two external legs, each of which are boson-type. Again, for any such graph we have by Lemma 5.1 and Euler's formula that $|V(\Gamma)| = f$, $p = \ell(\Gamma) - 1$ and $|V(\Gamma)| = 2p$; where p is the number of internal boson edges and f is the number of internal fermion edges.

By their definition, we see that these graphs are simply tadpoles with a distinguished fermion edge at which a *second* external boson leg is inserted.

REMARK 5.3. By the word 'second' above we literally mean that the roles of the two boson edges are physically different. This will be reflected in that we will always assume that one boson leg is the 'left' or 'first' one. For example, the graphs



are considered different even though one of them can be rotated to get the other one.

However, in the process of distinguishing a fermion edge of a tadpole, we have to exclude the fermion edge immediately before the tadpole's leg vertex as it will yield the same graph if the next fermion edge is chosen instead. Thus the generating function of these graphs, counted by the number of all boson edges is given by

$$(5.2) \quad U_{20}(x) = x(2xT'(x) - T(x)) = x(2xC'(x) - C(x)),$$

where T is as in Theorem 5.3, the generating function for Yukawa 1PI tadpoles counted by the number of all boson edges.

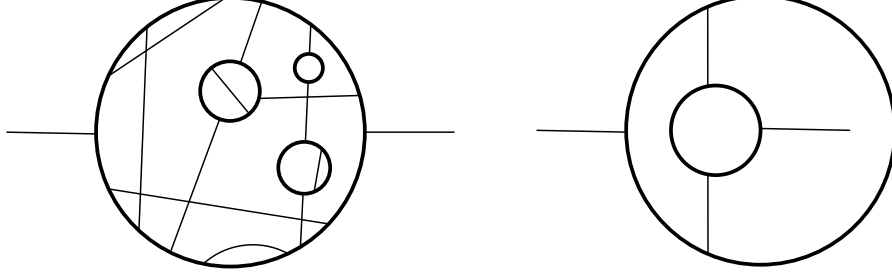


FIGURE 16. Two graphs generated by $\partial_{\phi_c}^2 (\partial_{\psi_c} \partial_{\bar{\psi}_c})^0 G^{\text{Yuk}}(\hbar, \phi_c, \psi_c) \Big|_{\phi_c = \psi_c = 0}$.

REMARK 5.4. Notice that the two boson legs are not necessarily on the same fermion loop, see the second graph in Figure 16 for example.

Thus, equation 5.2 shows that

$$(5.3) \quad [\hbar^n] \partial_{\phi_c}^2 (\partial_{\psi_c} \partial_{\bar{\psi}_c})^0 G^{\text{Yuk}}(\hbar, \phi_c, \psi_c) \Big|_{\phi_c = \psi_c = 0} = [x^{n+1}] U_{20}(x) = x(2xT'(x) - T(x))$$

$$(5.4) \quad = [x^n] (2xC'(x) - C(x)).$$

Further, by Proposition 2.2, it follows that

$$(5.5) \quad [\hbar^n] \partial_{\phi_c}^2 (\partial_{\psi_c} \partial_{\bar{\psi}_c})^0 G^{\text{Yuk}}(\hbar, \phi_c, \psi_c) \Big|_{\phi_c = \psi_c = 0} = [x^n] \frac{C(x)^2}{x} \left[\frac{C_{\geq 2}(t)}{t^2} \Big|_{t=C(x)^2/x} \right], \text{ or equivalently}$$

$$U_{20}(x) = C(x)^2 \left[\frac{C_{\geq 2}(t)}{t^2} \Big|_{t=C(x)^2/x} \right].$$

This equation will be useful in providing a chord-diagrammatic interpretation for graphs generated by $\partial_{\phi_c}^1 (\partial_{\psi_c} \partial_{\bar{\psi}_c})^1 G^{\text{Yuk}}(\hbar, \phi_c, \psi_c) \Big|_{\phi_c = \psi_c = 0}$, as we shall see next. For the next section we will need to give a name for the class of graphs considered here, and, as it became our good habit, we shall denote it by \mathcal{U}_{20} .

5.4. Yukawa Graphs from $\partial_{\phi_c}^1 (\partial_{\psi_c} \partial_{\bar{\psi}_c})^1 G^{\text{Yuk}}(\hbar, \phi_c, \psi_c) \Big|_{\phi_c = \psi_c = 0}$. These are the Yukawa 1PI graphs with vertex-type residue. Line 5 in Table 1 gives the number of these graphs, sized with loop number, up to size 5. These have two external fermion legs in addition to one boson leg (see Figure 17). Notice that if the ends of the two fermion external legs were identified we still wouldn't get a general

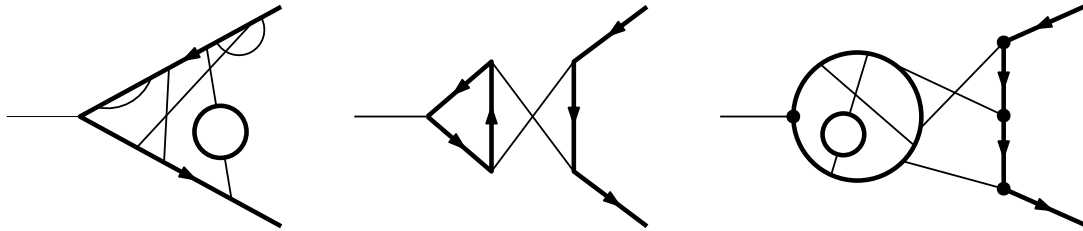


FIGURE 17. Examples of graphs generated by $\partial_{\phi_c}^1 (\partial_{\psi_c} \partial_{\bar{\psi}_c})^1 G^{\text{Yuk}}(\hbar, \phi_c, \psi_c) \Big|_{\phi_c = \psi_c = 0}$.

tadpole. The reason for this is that, since the graph is 1PI, we can not have something like the one in Figure 18 below. Knowing this is exactly the way we get the chord-diagrammatic interpretation.

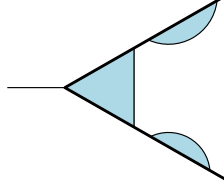
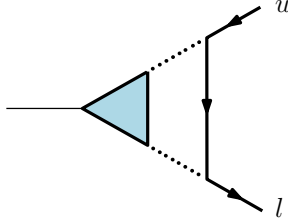


FIGURE 18. A forbidden graph.

We will let \mathcal{U}_{11} denote the class of all graphs generated by $\partial_{\phi_c}^1 (\partial_{\psi_c} \partial_{\bar{\psi}_c})^1 G^{\text{Yuk}}(\hbar, \phi_c, \psi_c) \Big|_{\phi_c = \psi_c = 0}$. Before proceeding to the next theorem recall that by Lemma 5.1 we have that for any $\Gamma \in \mathcal{U}_{11}$ $|V(\Gamma)| = f + 1$, and hence by Euler's formula $p = \ell(\Gamma)$, where f (and p) is the number of internal fermion (boson) edges.

NOTATION 5.2. In representing the graphs in \mathcal{U}_{11} , we still stick to the counter-clockwise convention, even for the unique path of fermion edges. We shall always represent the graphs in \mathcal{U}_{11} by fixing the boson external leg to the left, and then the fermion external half-edge directed towards the boson-leg vertex will be called the *upper end* and will be denoted with u_Γ ; on the other hand the fermion external half-edge directed away from the boson-leg vertex will be called the *lower end* and will be denoted by l_Γ .



THEOREM 5.6. Let \mathcal{U}_{11} be the class of Yukawa 1PI graphs (with vertex-type residue) generated by $\partial_{\phi_c}^1 (\partial_{\psi_c} \partial_{\bar{\psi}_c})^1 G^{\text{Yuk}}(\hbar, \phi_c, \psi_c) \Big|_{\phi_c = \psi_c = 0}$, and let $U_{11}(x)$ be the generating series of these graphs, counted by the number of all boson edges. Then

$$U_{11}(x) = x \frac{C_{\geq 2}(t)}{t^2} \Big|_{t=C(x)^2/x}.$$

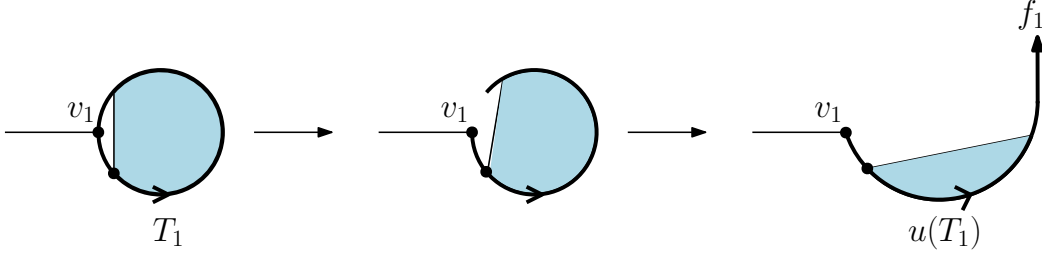
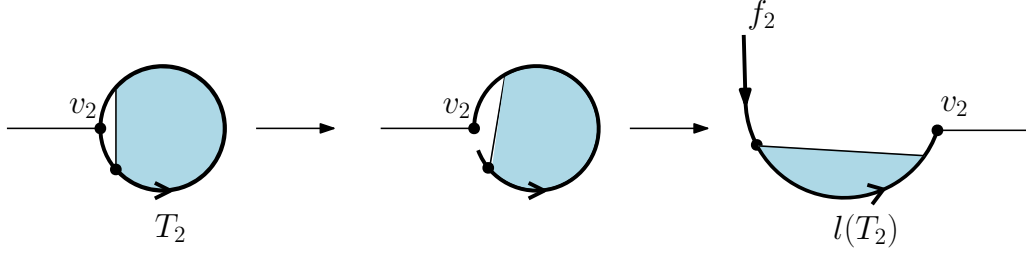
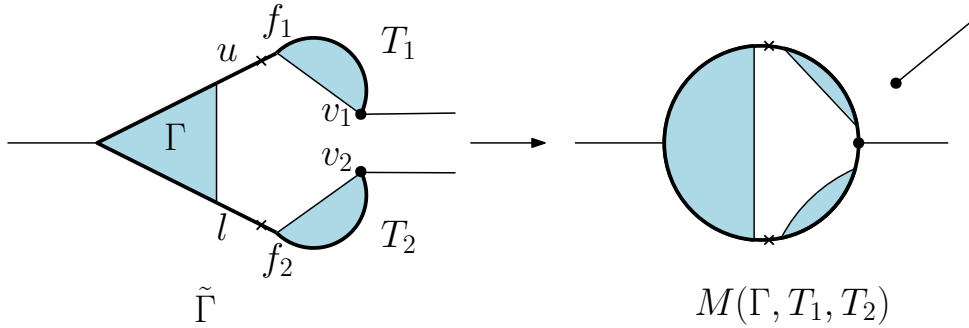
PROOF. We start with another type of graphs, namely with the class \mathcal{U}_{20} of the previous section. We will describe a bijection

$$M : \mathcal{U}_{11} * (\mathcal{U}_{10} * \mathcal{U}_{10}) \longrightarrow \mathcal{X} * \mathcal{U}_{20}.$$

The construction is simple: Assume $(\Gamma, (T_1, T_2))$ is a triplet from $\mathcal{U}_{11} * (\mathcal{U}_{10} * \mathcal{U}_{10})$. Let u and l be the upper and lower ends of Γ as described in Notation 5.2. Now take the tadpoles T_1 and T_2 and do the following:

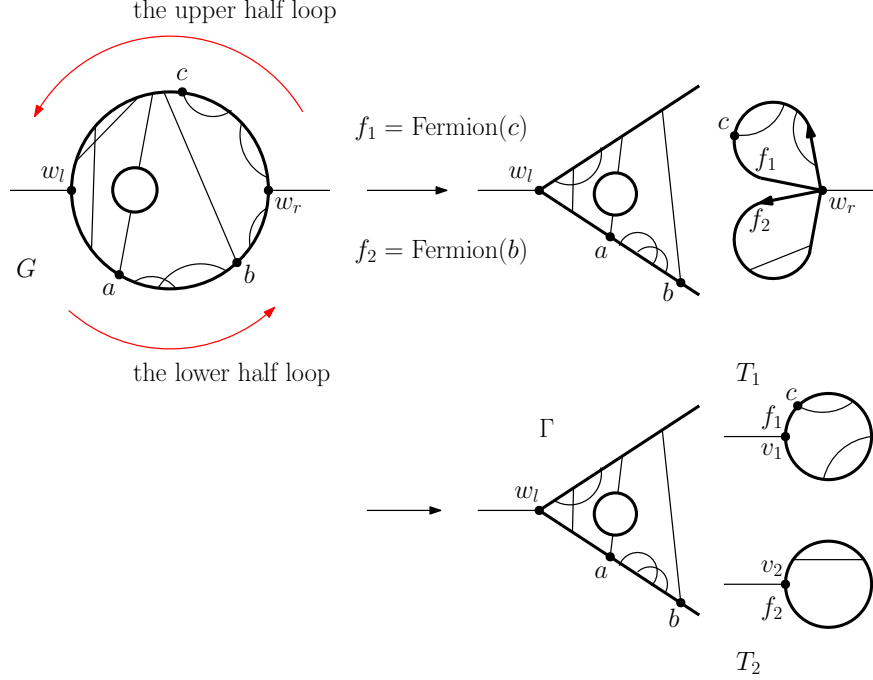
- (1) For T_1 , let v_1 be the vertex at the boson leg as before. Let f_1 be the fermion edge immediately before v_1 on $\text{Loop}(v_1)$. Detach f_1 from v_1 and denote the unique resulting graph with $u(T_1)$. This can be depicted as in Figure 19 below.
- (2) For T_2 , let v_2 be the vertex at the boson leg as before. Let f_2 be Fermion(v_2), the fermion edge immediately next to v_2 on $\text{Loop}(v_2)$. Detach f_2 from v_2 and denote the unique resulting graph with $l(T_2)$. This can be depicted as in Figure 20 below.
- (3) Identify f_1 with u of Γ and identify f_2 with l . Denote the resulting graph with $\tilde{\Gamma}$
- (4) Identify the vertices v_1 and v_2 in $\tilde{\Gamma}$.
- (5) By removing one of the external boson legs we get $M(\Gamma, T_1, T_2)$. The process described here can be depicted as in Figure 21 below.

By our construction, and by the uniqueness of the representation of graphs described in Notation 5.2, the map M described this way is well-defined. Moreover, it is reversible: Assume we are given a


 FIGURE 19. $u(T_1)$

 FIGURE 20. $l(T_2)$

 FIGURE 21. $M(\Gamma, T_1, T_2)$

graph G in \mathcal{U}_{20} in canonical representation (i.e. drawn according to our counter-clockwise convention). Remember from Remark 5.3, that the representation of G is unique and one boson leg is the ‘left’ external leg. Let w_l be and w_r be the corresponding vertices at the left and right boson legs respectively. Let us refer to the half fermion loop from w_r to w_l by the *upper half loop*, and similarly we will refer to the half fermion loop from w_l to w_r by the *lower half loop* (see Figure 22). Now we do the following:

- (1) Starting from w_r , remove $\text{Fermion}(w_r)$ from the graph G , and move along the rest of the upper half loop (direction is as before) searching for the **last** fermion edge whose removal disconnects $G - \text{Fermion}(w_r)$. Stop the search at w_l . Notice that it may happen that no such edge exists. If found, denote this edge by f_1 . If such an edge doesn’t exist we set $f_1 = \text{Fermion}(w_r)$.
- (2) Similarly, starting from w_l , remove $\text{Fermion}(w_l)$ from the graph G , and move along the rest of the lower half loop searching for the **first** fermion edge whose removal disconnects $G - \text{Fermion}(w_l)$. Stop the search at w_r . Notice that it may happen that no such edge exists. If found, denote this edge by f_2 . If such an edge doesn’t exist we set $f_2 =$ (fermion edge immediately before w_r).
- (3) Cut at f_1 and f_2 , and identify their ends with w_r such that the direction of f_1 with respect to w_r is counter-clockwise, whereas the direction of f_2 with respect to w_r is to be made clockwise.
- (4) Obtain T_1 and T_2 by splitting w_r and its boson leg into two copies. The remnant of G is Γ .

FIGURE 22. Calculating $M^{-1}(G)$.

It is worth noting that in Figure 22 f_2 is Fermion(b) and is not Fermion(a) as can be checked using the definition.

Thus, the map $M : \mathcal{U}_{11} * (\mathcal{U}_{10} * \mathcal{U}_{10}) \longrightarrow \mathcal{X} * \mathcal{U}_{20}$ is a bijection. Consequently, on the level of generating functions we will have

$$U_{11}(x)T(x)^2 = x U_{20}(x),$$

and hence, by equation (5.5) and Theorem 5.3, we get

$$U_{11}(x)C(x)^2 = x C(x)^2 \left[\frac{C_{\geq 2}(t)}{t^2} \Big|_{t=C(x)^2/x} \right],$$

that is,

$$(5.6) \quad U_{11}(x) = \frac{C_{\geq 2}(t)}{t^2} \Big|_{t=C(x)^2/x},$$

as desired. \square

5.5. Yukawa Graphs from $\partial_{\phi_c}^0 (\partial_{\psi_c} \partial_{\bar{\psi}_c})^1 G^{\text{Yuk}}(\hbar, \phi_c, \psi_c) \Big|_{\phi_c = \psi_c = 0}$. Let \mathcal{U}_{01} be the class of Yukawa 1PI graphs generated by $\partial_{\phi_c}^0 (\partial_{\psi_c} \partial_{\bar{\psi}_c})^1 G^{\text{Yuk}}(\hbar, \phi_c, \psi_c) \Big|_{\phi_c = \psi_c = 0}$. Line 4 in Table 1 gives the number of these graphs, sized with loop number, up to size 5. These are graphs with two external fermion legs and with no boson leg.

For any $\Gamma \in \mathcal{U}_{01}$, we have by Lemma 5.1 that $|V(\Gamma)| = f + 1$, and hence by Euler's formula $p = \ell(\Gamma)$, where f (and p) is the number of internal fermion (boson) edges. In particular,

$$(5.7) \quad f = 2p - 1.$$

We let $U_{01}(x)$ be the generating function of the graphs in \mathcal{U}_{01} counted by the number of boson edges.

There are two ways to think about this type of graphs, both can be used to obtain $U_{01}(x)$:

- (1) It is clear that the graphs in \mathcal{U}_{11} , which were considered in the last section, are the rooted versions of the graphs in \mathcal{U}_{01} , namely, except for the one-vertex graph, every graph in \mathcal{U}_{11} is

obtained from a unique graph in \mathcal{U}_{01} by distinguishing an internal fermion edge and inserting a boson leg. This means that, on the level of generating functions:

$$(5.8) \quad U_{11}(x) = x(2xU'_{01}(x) - U_{01}(x) + 1),$$

where the RHS uses the fact that $f = 2p - 1$ by equation (5.7), and where the 1 corresponds to the one-vertex graph in \mathcal{U}_{11} .

- (2) The other way is to think of a tadpole as being constructed from a list of graphs from \mathcal{U}_{01} . This way is more direct and we shall discuss it below.

PROPOSITION 5.7. *A Yukawa 1PI tadpole graph can be decomposed as boson leg together with a list of graphs from \mathcal{U}_{01} . In particular, on the level of generating functions we will have*

$$(5.9) \quad T(x) = \frac{x}{1 - U_{01}(x)}.$$

This in turn implies that

$$(5.10) \quad U_{01}(x) = 2xC'(x) - C(x) = C(x)^2 \left[\frac{C_{\geq 2}(t)}{t^2} \Big|_{t=C(x)^2/x} \right] = U_{20}(x).$$

PROOF. Given a tadpole $T \in \mathcal{U}_{10}$, we will give a unique decomposition into a boson leg together with a list of graphs from \mathcal{U}_{01} . Let v_T be the vertex at the boson external leg of T as usual. Also let f_0 be the fermion edge on $\text{Loop}(v_T)$ immediately before v_T .

- (1) If $f_0 = \text{Fermion}(v_T)$, return $(\text{---} \bullet; \emptyset)$.
- (2) Otherwise, detach f_0 and call the resulting graph $u(T)$.
- (3) Starting from v_T , move along $\text{Loop}(v_T)$ and determine all fermion edges on $\text{Loop}(v_T)$ whose removal disconnects $u(T)$. Let this list of fermion edges be

$$f_1, f_2, \dots, f_n.$$

(Note that it will always be the case that $f_1 = \text{Fermion}(v_T)$).

- (4) For $1 \leq i \leq n - 1$ define G_i to be the graph obtained from the original T by
 - cutting at f_i and f_{i+1} , and
 - deleting the component that contains v_T .
- (5) For $i = n$, define G_n to be the graph obtained from the original T by
 - cutting at f_n and f_0 , and
 - deleting the component that contains v_T .
- (6) Return $(\text{---} \bullet; G_1, G_2, \dots, G_n)$.

It is easily seen that the graphs G_i are 2-edge connected, in fact the graphs G_i are maximal 1PI's inserted along $\text{Loop}(v_T)$. Besides, by their definition, the graphs G_i have a fermion-type residue and are therefore in \mathcal{U}_{01} . Moreover, this construction is clearly unique for every tadpole in \mathcal{U}_{10} .

Conversely, every such list can be uniquely used to produce a tadpole. Figure 23 below illustrates two cases of this decomposition.

This gives that, on the level of generating functions,

$$T(x) = \frac{x}{1 - U_{01}(x)}.$$

By Lemma 2.1 recall that $C(x) = \frac{x}{1 - (2xC'(x) - C(x))}$, and since we have $T(x) = C(x)$ we get

$$U_{01}(x) = 2xC'(x) - C(x).$$

Then it follows from Proposition 2.2 that

$$U_{01}(x) = C(x)^2 \left[\frac{C_{\geq 2}(t)}{t^2} \Big|_{t=C(x)^2/x} \right] = U_{20}(x).$$

□

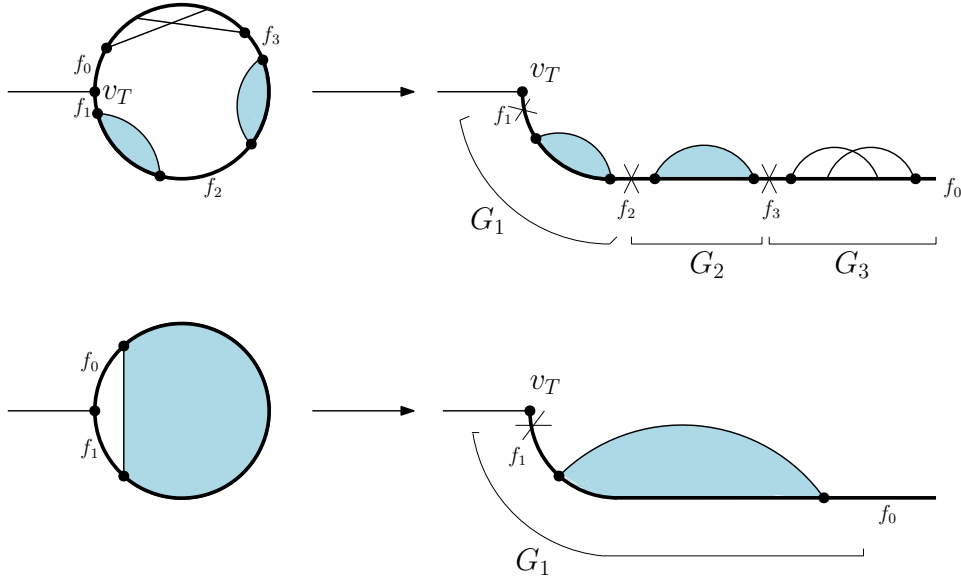


FIGURE 23. Examples of the decomposition of tadpoles into a list of graphs from \mathcal{U}_{01} .

Conclusion: We have thus obtained a chord-diagrammatic interpretation for a number of proper Green functions in Yukawa theory and quenched QED. In [2], the asymptotics of these generating series are obtained by means of singularity analysis. Here, having obtained every generating series in terms of connected chord diagrams, the task of obtaining the asymptotics is readily done and is a straightforward calculation now. Indeed, we only need to use our knowledge of $\mathcal{A}_{\frac{1}{2}}^2 C(x)$ (and $\mathcal{A}_{\frac{1}{2}}^2 C_{\geq 2}(x)$) to obtain the asymptotics for the different Yukawa and QED green functions considered here.

References

- [1] M. Borinsky. *Generating asymptotics for factorially divergent sequences*. arXiv preprint arXiv:1603.01236, 2016.
- [2] M. Borinsky. *Renormalized asymptotic enumeration of Feynman diagrams*. *Annals Phys.* 385 (2017) 95-135, DOI: 10.1016/j.aop.2017.07.009, 2017.
- [3] M. Borinsky. *Graphs in perturbation theory: Algebraic structure and asymptotics*. arXiv:1807.02046, 2018.
- [4] M. Borinsky. *Algebraic lattices in QFT renormalization*. *Letters in Mathematical Physics*, Volume 106, Issue 7, pp 879-911, arXiv:1509.01862, July 2016,.
- [5] A. Connes and D. Kreimer. *Renormalization in quantum field theory and the Riemann–Hilbert problem i: The Hopf algebra structure of graphs and the main theorem*. *Communications in Mathematical Physics*, 210:249–273, 2000.
- [6] J. Courtiel, K. Yeats, and N. Zeilberger. *Connected chord diagrams and bridgeless maps*. arXiv:1611.04611, 2017.
- [7] P. Cvitanović, B. Lautrup, and R. B. Pearson. *Number and weights of Feynman diagrams*. *Phys. Rev. D* Vol. 18 (6), 1978.
- [8] P. Flajolet and M. Noy. *Formal Power Series and Algebraic Combinatorics: 12th International Conference, FPSAC'00, Moscow, Russia, June 2000, Proceedings*. *Journal of Algorithms*, pp. 191–201, Berlin, Heidelberg: Springer Berlin Heidelberg, 2000.
- [9] D. M. Jackson, A. Kempf, and A. Morales. *Algebraic Combinatorial fourier and Legendre Transforms with Application in Perturbative Quantum Field Theory*. arXiv:1805.09812v3, 2019.
- [10] A. A. Mahmoud. *An Asymptotic Expansion for the Number of 2-Connected Chord Diagrams*. *Journal of Mathematical Physics* (Vol.64, Issue 12), DOI: 10.1063/5.0171074, 2023.
- [11] D. Manchon. *Hopf algebras, from basics to applications to renormalization*. arXiv preprint math/0408405, 2004.